Available online at www.sciencedirect.com
ScienceDirect
Journal of Power Sources 179 (2008) 357–360
JOURNAL OF POWER SOURCES
www.elsevier.com/locate/jpowsour

Short communication

MoO_2 synthesized by reduction of MoO_3 with ethanol vapor as an anode material with good rate capability for the lithium ion battery

L.C. Yang [a], Q.S. Gao [a], Y. Tang [a], Y.P. Wu [a,*], R. Holze [b,**]

[a] *Department of Chemistry and Shanghai Key Laboratory of Molecular Catalysis & Innovative Materials, Fudan University, Shanghai 200433, China*
[b] *Institut für Chemie, AG Elektrochemie, Technische Universität Chemnitz, D-09111 Chemnitz, Germany*

Received 28 September 2007; received in revised form 11 December 2007; accepted 24 December 2007
Available online 5 January 2008

Abstract

MoO_2 synthesized through reduction of MoO_3 with ethanol vapor at 400 °C was characterized by X-ray diffraction (XRD), scanning electron microscopy (SEM) and transmission electron microscopy (TEM). Its electrochemical performance as an anode material for lithium ion battery was tested by cyclic voltammetry (CV) and capacity measurements. During the reduction process, the starting material (MoO_3) collapsed into nanoparticles (~100 nm), on the nanoparticles remains a carbon layer from ethanol decomposition. Rate capacity and cycling performance of the as-prepared product is very satisfactory. It displays 318 mAh g^{-1} in the initial charge process with capacity retention of 100% after 20 cycles in the range of 0.01–3.00 V vs. lithium metal at a current density of 5.0 mA cm^{-2}, and around 85% of the retrievable capacity is in the range of 1.00–2.00 V. This suggests the application of this type of MoO_2 as anode material in lithium ion batteries.

Keywords: Lithium ion battery; MoO_2; MoO_3; Alcohol vapor reduction

1. Introduction

Up to now, lithium ion batteries are widely used in a range of portable electronic devices, including mobile phones, laptop computers and video cameras [1–3]. To expand the application fields of lithium ion batteries towards electric vehicles in the automotive industry, there is a need to improve the rate capability of the batteries to get high power density. Utilization of nanostructured materials with small particle size and large surface area is thought to be one solution since the diffusion distance for lithium ions and the true current density are greatly decreased [4–6]. It is demonstrated that the rate capabilities of nanostructured SnO_2 and V_2O_5 electrodes are improved compared with the corresponding thin film-based electrodes [7–9]. Nanostructured TiO_2 also exhibits rate capability superior to their bulk counterparts [10–12]. It seems safe to conclude, that the improved rate capability is associated with larger surface area and shorter diffusion path lengths in the nanostructured materials.

Many of the rutile-related transition metal oxides can be intercalated with lithium at room temperature. Of these, MoO_2, with good electronic conductivity, is a promising anode material, which can incorporate lithium ions into its lattice structure during charge and provides a reversible storage source for lithium ions [13–15]. Traditionally, MoO_2 is prepared by reducing MoO_3 with hydrogen at high temperature [16–18]. Here we use ethanol vapor as a reducing agent instead of hydrogen, which is much cheaper and safer. The results demonstrate that MoO_2 collapses into nanoparticles during the reduction process when oxygen is released from the lattice, and that the nanoparticles are coated with a carbon layer generated from ethanol decomposition, which is beneficial for high rate capability and cycleability.

2. Experimental

The experimental setup used for preparing MoO_2 through ethanol vapor reduction is presented in Fig. 1. A ceramic boat containing about 1.0 g MoO_3 was put into the furnace, and the

* Corresponding author.
** Corresponding author. Tel.: +49 371 531 21260; fax: +49 371 531 21269.
E-mail addresses: wuyp@fudan.edu.cn (Y.P. Wu), rudolf.holze@chemie.tu-chemnitz.de (R. Holze).

0378-7753/$ – see front matter © 2008 Elsevier B.V. All rights reserved.
doi:10.1016/j.jpowsour.2007.12.099

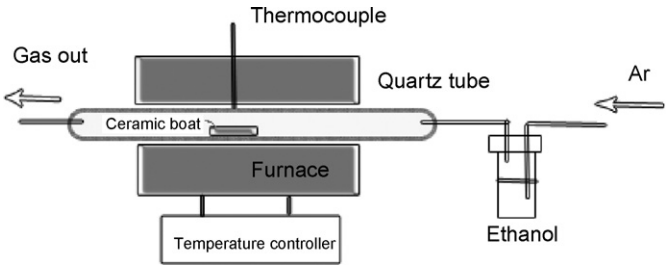

Fig. 1. Schematic drawing of the setup used for MoO_2 preparation.

vaporized ethanol was carried by an argon flow (50 ml min^{-1}). After complete removal of the air in the quartz tube by flushing argon for 4 h, MoO_3 was calcinated at 400 °C for 12 h under the Ar/ethanol vapor flow.

X-ray diffraction (XRD) pattern of the product was recorded on a Bruker Advance 8 diffractometer with monochromatized Cu Kα radiation (λ = 1.5406 Å). Scanning electron microscopic (SEM) and transmission electron microscopic (TEM) images were obtained on a Philips XL 30 scanning electron microscope and a JEOL JEM-2010 transmission electron microscope, respectively.

The electrochemical performance of the as-obtained MoO_2 was tested as the anode for lithium ion battery. To prepare the composite electrode, 80% active mass (as-prepared MoO_2), 10% carbon black and 10% poly(vinylidene difluoride) (PVdF) were mixed and then suspended in *N*-methylpyrrolidone to make a slurry that spreads uniformly on a copper foil current collector. The coated copper foil was cut into pieces with a diameter of 1 cm, dried under ambient condition and subsequently at 120 °C in vacuum overnight. Finally, model button cells were assembled in a glove box with lithium foil as the counter and reference electrode, Celgard 2400 as the separator, and LIB315 (a standard 1 M LiF_6 solution in a 1:1:1 mixture of EC, DMC and DEC, Guotai Huarong Chemical Plant) as the electrolyte solution. CV was measured using a CHI 600C electrochemistry work station (Shanghai CH Instruments). Galvanostatic cycling was performed using LANDct3.3 battery tester.

3. Results and discussion

The XRD pattern of the as-prepared product is shown in Fig. 2. All diffraction peaks can be assigned to those of MoO_2 with monoclinic symmetry (JCPDS, No. 32–0671). No peaks of MoO_3 or other molybdenum oxides are observed. This indicates that MoO_3 was completely reduced by ethanol vapor to single phase MoO_2 with monoclinic symmetry.

The SEM images of the starting material MoO_3 and the as-prepared MoO_2 are presented in Fig. 3. As for the product MoO_2, grains of nanometer size appear, the surface of the product became coarse compared with that of the parent oxide. From the TEM images (Fig. 4), more details can be observed. Fig. 4a indicates that the starting material was finally broken into nanoparticles (about 100 nm) as the oxygen was released from the lattice when the reduction took place. Moreover, Fig. 4b shows that over the nanoparticle there is a layer of nanometer

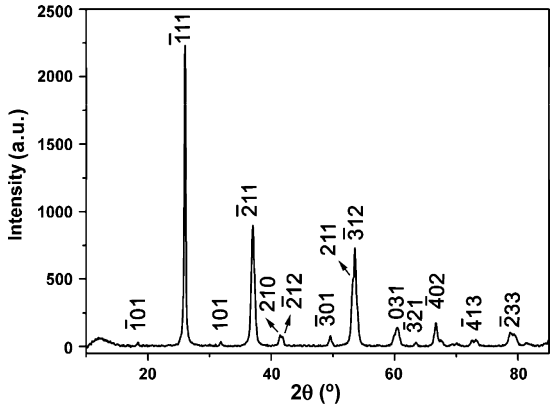

Fig. 2. XRD pattern of the as-prepared MoO_2.

thickness with an observed interplanar spacing of about 0.36 nm corresponding to the separation between (0 0 2) lattice planes of graphite. Evidently, the nano-carbon layer is generated from the pyrolysis of ethanol vapor. The carbon yield is too small to be observed by XRD because the temperature (400 °C) is comparatively low.

The first four consecutive cyclic voltammograms of the as-prepared MoO_2 are depicted in Fig. 5. The first cycle reflects irreversible cathodic charge, which may be related to the reduc-

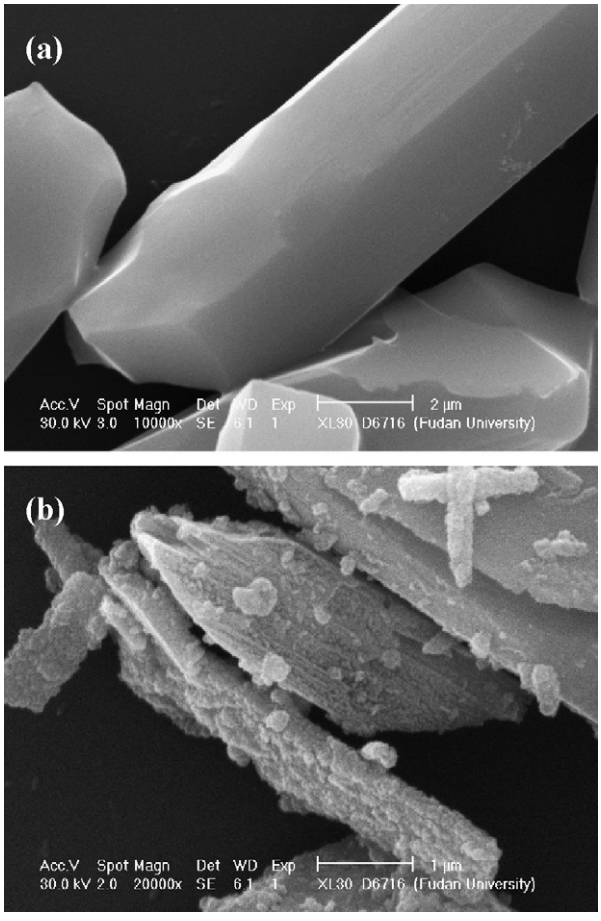

Fig. 3. SEM images of (a) the starting material MoO_3 and (b) the as-prepared MoO_2.

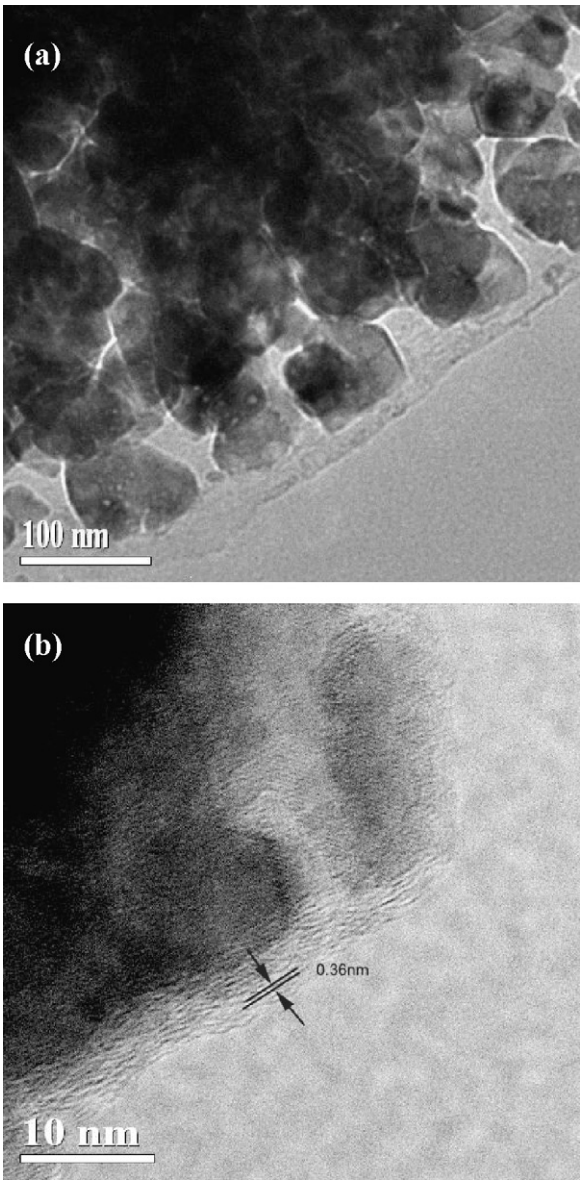

Fig. 4. TEM images of the as-obtained MoO_2 at different magnifications.

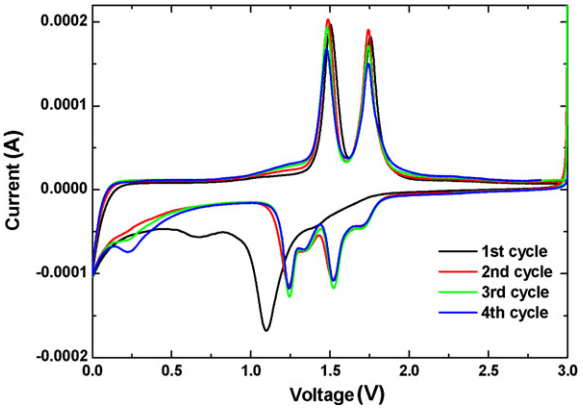

Fig. 5. Cyclic voltammograms (CVs) of the MoO_2 electrodes measured in the voltage range of 0–3.0 V with a scan rate of 0.05 mV s^{-1} for the first four consecutive cycles.

tion of solution species and formation of a passivating surface film on the anode (see the small peak at about 0.6 V). In the subsequent cycles, a reversible insertion of lithium is obtained with coulombic efficiency close to 100%. Obviously, there are two redox couples at 1.24/1.49 and 1.52/1.74 V, respectively. The separation between reduction and oxidation peaks (ΔE) is small and the cyclic voltammetry (CV) curves for the 2nd to 4th cycle highly overlap, which demonstrates that the as-prepared product has good stability and reversibility for lithium ion insertion and extraction.

The initial discharge–charge profiles of the as-obtained MoO_2 recorded at the current density of 5.0 mA cm^{-2} and the cycling behavior within twenty cycles are shown in Fig. 6. There are two potential plateaus at around 1.2 and 1.5 V on discharge as well as 1.5 and 1.8 V on charge, which is in agreement with the redox peaks observed in the CVs. Based on previous research, the inflection point between these plateaus represents a transition between monoclinic phase and orthogonal phase in the partially lithiated oxide Li_xMoO_2 [19,20]. In the first cycle, the discharge capacity is 417 mAh g^{-1}, and the charge capacity is 318 mAh g^{-1}, with a coulombic efficiency of 76.3% due to the irreversible capacity associated with the decomposition of the electrolyte solution and the SEI formation. In the subsequent cycles, the coulombic efficiency is nearly 100%, the charge capacity remains around 320 mAh g^{-1} with no capacity fading

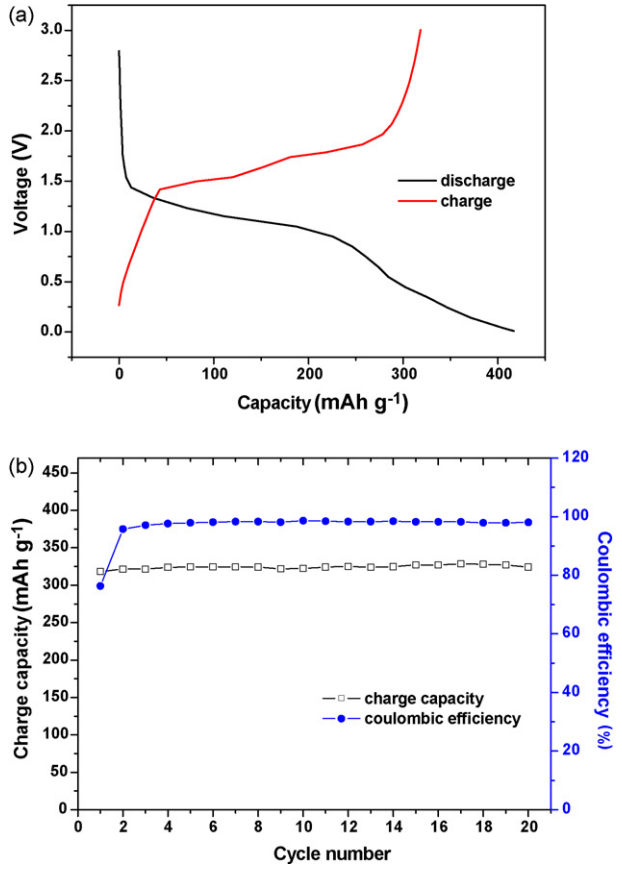

Fig. 6. (a) Charge/discharge profiles for the first cycle and (b) cycling behavior of the as-obtained MoO_2 tested in the range of 0.01–3.00 V vs. metallic lithium at a current density of 5.0 mA cm^{-2}.

after 20 cycles in the range of 0.01–3.00 V vs. lithium metal, and around 85% of the retrievable (reversible) capacity is within the range of 1.00–2.00 V.

The as-prepared MoO_2 exhibits excellent cycleability under high current density, which is due to the good conductivity of MoO_2 and nanoparticular structure generated during reduction of MoO_3 with high surface area that reduce the actual effective current density on the active material. Furthermore, the carbon layer on the nanoparticles can enhance the conductivity and prevent the nanoparticles from aggregating, which ensures the good cycleability of the as-prepared product, which is similar to the behavior of carbon coatings observed elsewhere [21,22].

4. Conclusions

MoO_2 as suitable anode materials for lithium rechargeable batteries was prepared through reducing MoO_3 with ethanol vapor. MoO_3 collapsed into nanoparticles (∼100 nm) with a coating of a carbon layer generated by ethanol decomposition. When discharged and charged at a current density as high as 5.0 mA cm^{-2}, the activated MoO_2 displays reversible capacity of 318 mAh g^{-1} in the initial charge process with a capacity retention of 100% after 20 cycles. These results suggest that this type of MoO_2 obtained by ethanol vapor reduction can be a promising anode material with high rate capability for rechargeable lithium ion batteries.

Acknowledgements

Financial support from National Basic Research Program of China (973 Program No.: 2007CB209700), STCSM (04QMX1406, 06DJ14006 and 0552 nm05025) and NSFC (50573012, 20421303) is greatly appreciated.

References

[1] P. Poizot, S. Laruelle, S. Grugeon, L. Dupont, J.M. Tarascon, Nature 407 (2000) 496–499.
[2] D. Souza, V. Pralong, A.J. Jacobson, L.F. Nazar, Science 296 (2002) 2012–2015.
[3] Y.P. Wu, X.B. Dai, J.Q. Ma, Y.J. Chen, Lithium Ion Batteries—Practice and Applications, Chemical Industry Press, 2004.
[4] P.R. Bueno, E.R. Leite, J. Phys. Chem. B 107 (2003) 8868–8877.
[5] H. Habazaki, M. Kiriu, H. Konno, Electrochem. Commun. 8 (2006) 1275–1279.
[6] P.L. Taberna1, S. Mitra, P. Poizot, P. Simon, J.M. Tarascon, Nat. Mater. 5 (2006) 567–573.
[7] C.R. Sides, C.R. Martin, Adv. Mater. 17 (2005) 125–128.
[8] C.J. Patrissi, C.R. Martin, J. Electrochem. Soc. 148 (2001) A1247–A1253.
[9] N.C. Li, C.R. Martin, B. Scrosati, J. Power Sources 97 (8) (2001) 240–243.
[10] Y.S. Hu, L. Kienle, Y.G. Guo, J. Maier, Adv. Mater. 18 (2006) 1421–1426.
[11] A.R. Armstrong, G. Armstrong, J. Canales, R. Garcia, P.G. Bruce, Adv. Mater. 17 (2005) 862–865.
[12] L.J. Fu, T. Zhang, Q. Cao, H.P. Zhang, Y.P. Wu, Electrochem. Commun. 9 (2007) 2140–2144.
[13] Y.G. Liang, S.J. Yang, Z.H. Yi, J.T. Sun, Y.H. Zhou, Mater. Chem. Phys. 93 (2005) 395–398.
[14] J.J. Auborn, Y.L. Barberio, J. Electrochem. Soc. 134 (1987) 638–641.
[15] L.C. Yang, Q.S. Gao, Y.H. Zhang, Y. Tang, Y.P. Wu, Electrochem. Commun. 10 (2008) 118–122.
[16] B.C. Satishkumar, A. Govindaraj, M. Nath, C.N.R. Rao, J. Mater. Chem. 10 (2000) 2115–2119.
[17] P. Wehrer, C. Bigey, L. Hilaire, Appl. Catal. A Gen. 243 (2003) 109–119.
[18] A. Katrib, J.W. Sobczak, M. Krawczyk, L. Zommer, A. Benadda, A. Jablonski, G. Maire, Surf. Interface Anal. 34 (2002) 225–229.
[19] J.R. Dahn, W.R. Mckinnon, Solid State Ionics 23 (1987) 1–7.
[20] Y.G. Liang, S.J. Yang, Z.H. Yi, X.F. Lei, J.T. Sun, Y.H. Zhou, Mater. Sci. Eng. B 121 (2005) 152–155.
[21] L.J. Fu, H. Liu, H.P. Zhang, C. Li, T. Zhang, Y.P. Wu, R. Holze, H.Q. Wu, Electrochem. Commun. 8 (2006) 1–4.
[22] T. Zhang, L.J. Fu, J. Gao, L.C. Yang, Y.P. Wu, H.Q. Wu, Pure Appl. Chem. 78 (2006) 1889–1896.